

# Interface roughening in Hele-Shaw flows with quenched disorder: Experimental and theoretical results

A. HERNÁNDEZ-MACHADO<sup>1,2</sup>(\*), J. SORIANO<sup>1</sup>, A. M. LACASTA<sup>3</sup>, M. A. RODRÍGUEZ<sup>4</sup>,  
L. RAMÍREZ-PISCINA<sup>3</sup> and J. ORTÍN<sup>1</sup>

<sup>1</sup> Departament ECM, Facultat de Física, Universitat de Barcelona  
Diagonal 647, E-08028 Barcelona, Spain

<sup>2</sup> Groupe de Physique des Solides, Université Pierre-et-Marie-Curie  
Tour 23, 2 place Jussieu, 75251 Paris Cedex 05, France

<sup>3</sup> Departament de Física Aplicada, Universitat Politècnica de Catalunya  
Avda. Dr. Marañón 44, E-08034 Barcelona, Spain

<sup>4</sup> Instituto de Física de Cantabria, CSIC  
Avenida Los Castros, E-39005 Santander, Spain

(received 22 November 2000; accepted in final form 14 May 2001)

PACS. 47.55.Mh – Flows through porous media.

PACS. 68.35.Ct – Interface structure and roughness.

PACS. 05.40.-a – Fluctuation phenomena, random processes, noise, and Brownian motion.

**Abstract.** – We study the forced fluid invasion of an air-filled model porous medium at constant flow rate, in  $1 + 1$  dimensions, both experimentally and theoretically. We focus on the nonlocal character of the interface dynamics, due to liquid conservation, and its effect on the scaling properties of the interface upon roughening. Specifically, we study the limit of large flow rates and weak capillary forces. Our theory predicts a roughening behaviour characterized at short times by a growth exponent  $\beta_1 = 5/6$ , a roughness exponent  $\alpha_1 = 5/2$ , and a dynamic exponent  $z_1 = 3$ , and by  $\beta_2 = 1/2$ ,  $\alpha_2 = 1/2$ , and  $z_2 = 1$  at long times, before saturation. This theoretical prediction is in good agreement with the experiments at long times. The ensemble of experiments, theory, and simulations provides evidence for a new universality class of interface roughening in  $1 + 1$  dimensions.

Studies on the morphology of interfaces moving in disordered media under nonequilibrium conditions constitute an active field of research [1]. One relevant example is the forced invasion of an air-filled porous medium by a viscous wetting fluid such as oil or water, which gives rise to a nonequilibrium rough interface [2–6]. The roughening process of an initially flat interface is described in terms of the interfacial root-mean-square width  $w$ . In many systems  $w$  follows a Family-Vicsek dynamical scaling [7]:  $w \sim t^\beta$  for  $t < t_x$ ,  $w \sim L^\alpha$  for  $t > t_x$  and  $t_x \sim L^z$ , with  $\alpha = z\beta$ . Here  $t_x$  is a saturation time,  $\beta$  the growth exponent,  $\alpha$  the roughness exponent, and  $z$  the dynamic exponent. The roughness exponent can also be obtained from the power spectrum

---

(\*) E-mail: aurora@ecm.ub.es

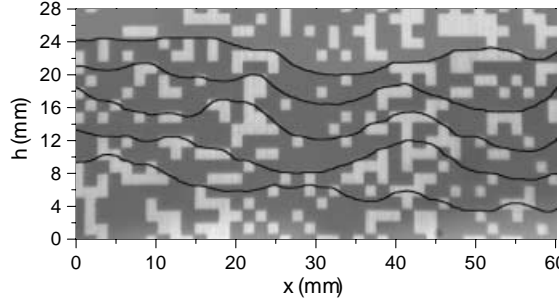


Fig. 1 – Several consecutive close-up views of a piece of the oil-air interface, taken at 150 s time intervals. The flow rate is  $Q = 10 \text{ ml/h}$ .

$S(q, t)$ , which is less sensitive to finite-size effects. We have [8]  $S(q, t) = q^{-(2\alpha+1)} s_{\text{FV}}(qt^{1/z})$ , where  $s_{\text{FV}}$  obeys  $s_{\text{FV}}(u) \sim \text{const}$  when  $u \gg 1$ , and  $s_{\text{FV}}(u) \sim u^{2\alpha+1}$  when  $u \ll 1$ .

Experiments of forced fluid invasion (FFI) in air-filled packings of glass beads, in  $1 + 1$  dimensions, have given roughness exponents in the range  $\alpha = 0.6\text{--}0.9$  [2–5]. The dispersion reflects the fact that the effective values of  $\alpha$ , determined by measuring widths over several scales at saturation, depend on the capillary number  $C_a$  [4]. On the other hand, there are few experimental determinations of the exponent  $\beta$ , because the large relative strength of capillary to viscous forces made the growth regime extremely short in most experiments.

In this letter we report new experimental results of dynamic interfacial roughening in FFI, in  $1 + 1$  dimensions, at *constant injection rate*. In our case the model porous medium is a Hele-Shaw cell with controlled spatial fluctuations of the gap thickness. While the viscous pressure field and the surface tension in the plane of the cell keep the interface smooth on large length scales, fluctuations in the gap thickness produce local fluctuations in capillary pressure which roughen the interface. Thus the governing physics is the same as in a real two-dimensional porous medium, and we have the possibility of controlling the statistical properties and the relative strength of the disorder.

In our experiments a silicone oil [9] displaces air in a horizontal Hele-Shaw cell,  $190 \times 550 \text{ mm}^2$ , made of two glass plates 19 mm thick. Fluctuations in the gap thickness are provided by a fiber glass substrate which contains a random distribution of square copper islands filling 35% of the substrate. Each island is  $0.06 \pm 0.01 \text{ mm}$  thick and has  $1.500 \pm 0.005 \text{ mm}$  lateral size (fig. 1). The gap spacing from the substrate to the top plate is  $b = 0.36 \pm 0.05 \text{ mm}$ . Since the maximum width of the meniscus is only one half the gap width, the interface can be considered one-dimensional at the length scale of the copper islands. The oil is injected at one side of the cell using a constant flow rate syringe pump. A flat front is first prepared by keeping the oil at rest in a transverse copper track separated 2 mm from the beginning of the noise. Initially the oil is pushed at high flow rate (300 ml/h) for about 4 s to keep the interface smooth while it enters the noise. Next, at a time defined as  $t = 0$ , the flow rate is set to its nominal value  $Q$ , and the oil-air interface is monitored as a function of time using two CCD cameras, with a final spatial resolution of 0.37 mm/pixel. This imposes a cut-off at small length scales, about twice the maximum width of the meniscus. We choose a range of flow rates ( $10 \leq Q \leq 100 \text{ ml/h}$ ) such that the contact line overcomes the copper islands rather easily, without pinning or forming overhangs. For  $Q = 10 \text{ ml/h}$  (fig. 1) the average interface velocity is  $v = 0.038 \pm 0.005 \text{ mm/s}$ , which we take as a reference.

Our results for  $w(t)$  are presented in fig. 2(a). As expected, both the saturation time and the interfacial width  $w$  at saturation depend on the average velocity at which the interface

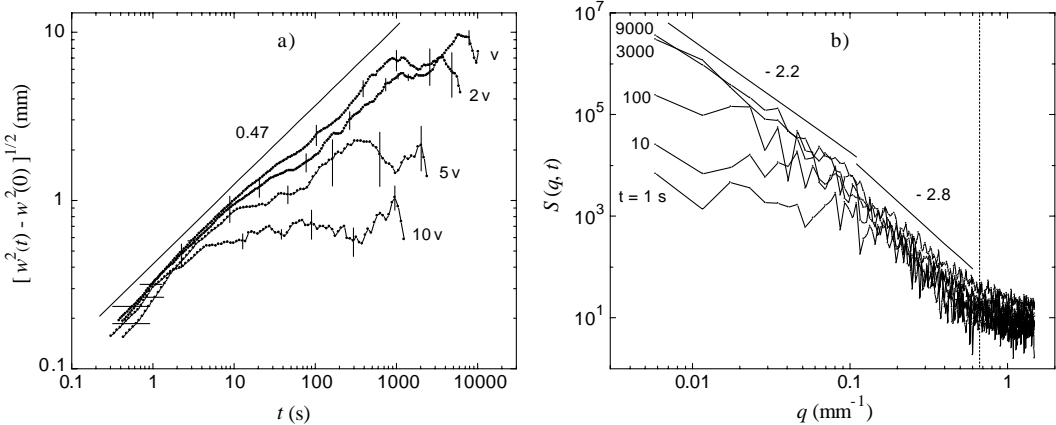


Fig. 2 – a) Double-logarithmic plot of  $w(t)$  for four different interface velocities. Each curve is an average over 6 experiments (3 runs on 2 different realizations of the noise). In each experiment  $w^2(0)$  has been subtracted from  $w^2(t)$ , in order to minimize the effect of the initial condition. The error bars give a measure of the overall dispersion between different experiments. b) Power spectrum of the interface profiles at successive time intervals, for the experiments at velocity  $v$ . The vertical line indicates the spatial scale of the disorder.

is driven. We observe also large fluctuations in the interfacial width, consistent with the observations reported in [4]. The fluctuations in  $w$  are highly reproducible in experimental runs with the same realization of the disorder. Disregarding fluctuations, the growth of the interfacial width is consistent with a power law  $w \sim t^\beta$ , with  $\beta = 0.47 \pm 0.04$ , extending about three orders of magnitude in  $t$  (for measurements at velocity  $v$ ) until the width saturates.

The power spectrum for the set of measurements at velocity  $v$  is shown in fig. 2(b). At short times the spectrum displays a *plateau* for small  $q$  and a power law decay at large  $q$  as expected. As the interface advances in the disorder the value of the *plateau* increases, and we observe the emergence of another scale-independent (power law) behaviour for an increasingly growing range of spatial scales, in agreement with the scaling of  $S(q,t)$  expected for  $u = qt^{1/z} \ll 1$ . This behaviour is also observed at velocity  $2v$ . The measured exponents are  $-2.2 \pm 0.2$  ( $\alpha = 0.6 \pm 0.1$ ) at small  $q$  (long length scales) and  $-2.8 \pm 0.2$  ( $\alpha = 0.9 \pm 0.1$ ) at large  $q$  (short length scales). The spectra of the experimental interfaces have been calculated imposing periodic boundary conditions. To this purpose, we have subtracted from the interface the straight line joining its two ends. This correction eliminates an artificial slope that is specially important at saturation, where the difference in height between the two ends is maximum [10].

One interesting aspect of roughening in fluid flows is the *nonlocal* nature of the interfacial dynamics, due to liquid conservation. The importance of nonlocality in this problem has been already pointed out by a number of authors [4, 6, 11]. Very recently, this issue has been addressed explicitly in the theoretical formulation of FFI at constant pressure [12] and of spontaneous imbibition [12, 13]. In this letter we address the same issue for FFI at constant flow rate. This driving condition has not been explored theoretically yet, in spite of being often used in experiments.

Our model is based on a time-dependent Ginzburg Landau model with conserved order parameter (model B in ref. [14]):

$$\frac{\partial \phi}{\partial t} = \nabla M \nabla (-\phi + \phi^3 - \epsilon^2 \nabla^2 \phi). \quad (1)$$

$\phi$  is the order parameter with equilibrium values  $\phi_{\text{eq}} = \pm 1$ , and  $\epsilon$  is the interfacial width.  $M$  is the mobility, which we consider fluctuating in space:

$$M(\phi, \mathbf{r}) = \begin{cases} K(1 + \xi(\mathbf{r})) & \text{for oil } (\phi > 0), \\ 0 & \text{for air } (\phi < 0), \end{cases} \quad (2)$$

with  $K$  a macroscopic mobility and  $\xi(\mathbf{r})$  a weak static disorder with a spatial correlation:

$$\langle \xi(\mathbf{r})\xi(\mathbf{r}') \rangle = 2DC \left( \frac{|\mathbf{r} - \mathbf{r}'|}{\lambda} \right), \quad (3)$$

where  $\lambda$  is the disorder correlation length and  $C$  is normalized. Dubé *et al.* [13] have proposed a similar formulation for spontaneous imbibition. In their problem the interface is driven only by capillary forces, and moves with average velocity  $\bar{v} \sim t^{-1/2}$ . Here, instead, nonlocal viscous forces are dominant over the local fluctuations of capillary pressure: our interface is driven by a constant flux  $\gamma_0$ , which gives rise to a steady-state rough interface moving with constant noise-dependent  $\bar{v}$ . The disorder is also introduced differently in the two approaches. In our two-dimensional model the fluctuations in gap thickness are represented (phenomenologically) by a fluctuating mobility.

The macroscopic limit of the model is obtained by an asymptotic expansion in orders of  $\epsilon$ , following a procedure described in ref. [15]:

$$\begin{aligned} \nabla(1 + \xi(\mathbf{r}))\nabla P &= 0, \\ P &= -\Gamma\kappa, \\ v_n &= -K(1 + \xi(x, y_{\text{int}}))(\nabla P)_n, \end{aligned} \quad (4)$$

where the pressure field in the bulk of the liquid is given by  $P = (\phi(\mathbf{r}, t) - \phi_{\text{eq}})/(2\phi_{\text{eq}})$ , the surface tension is given by  $\Gamma = (2\phi_{\text{eq}})^{-2} \int dy (\partial_y \phi_{\text{st}})^2$ ,  $\phi_{\text{st}}$  is the steady planar solution of eq. (1),  $\kappa$  is the curvature of the interface, and  $v_n$  its normal velocity.  $\xi(x, y_{\text{int}})$  is taken at the interface. The deterministic part of eq. (4) reproduces the macroscopic equations for oil-air displacements in a Hele-Shaw cell [16].

The interfacial equation in Fourier space can be derived from eq. (4) using Green function analysis. We define  $\bar{P} = P + \bar{\gamma}_0/K(y - \bar{\gamma}_0 t)$ , where  $\bar{\gamma}_0 = \gamma_0/(4\phi_{\text{eq}})$ . In this case, the Green function  $G(\mathbf{r}, \mathbf{r}')$  obeys  $\nabla^2 G = \delta(\mathbf{r} - \mathbf{r}')$ . The interfacial equation for the local deviations of the interface from its mean position,  $h(x, t) = y_{\text{int}} - \bar{v}t$ , reads (to first order in  $\xi$ ):

$$\begin{aligned} \int ds' G(s, s') \frac{v_n(s') - \bar{\gamma}_0 \hat{n} \hat{y}}{K} &= \frac{1}{2} \left[ -\Gamma\kappa(s) + \frac{\bar{\gamma}_0}{K} (h(s) + (\bar{v} - \bar{\gamma}_0)t) \right] + \\ + \int ds' \hat{n} \nabla G(s, s') \left[ -\Gamma\kappa(s') + \frac{\bar{\gamma}_0}{K} (h(s') + (\bar{v} - \bar{\gamma}_0)t) \right] &+ \int ds' G(s, s') \frac{v_n}{K} \xi(s', y_{\text{int}}), \end{aligned} \quad (5)$$

where  $s$  is the contour variable on the interface and  $\hat{n}$  and  $\hat{y}$  are the unitary vectors perpendicular to the interface and along the  $y$ -direction, respectively. We have neglected volume terms which do not contribute to the scaling. A distinguishing feature of eq. (5) is the presence of integral terms, which account for the *nonlocal* character of the interfacial dynamics. The deterministic part is equivalent to the equation for unstable displacements (air displacing oil,  $\bar{\gamma}_0 < 0$ ) derived in refs. [17, 18].

In this problem, due to the presence of a correlated disorder, two different time scales of dynamic origin are present. One of them is related to the ballistic dynamics of the interface due to the driving and corresponds to the time in which the interface advances the noise

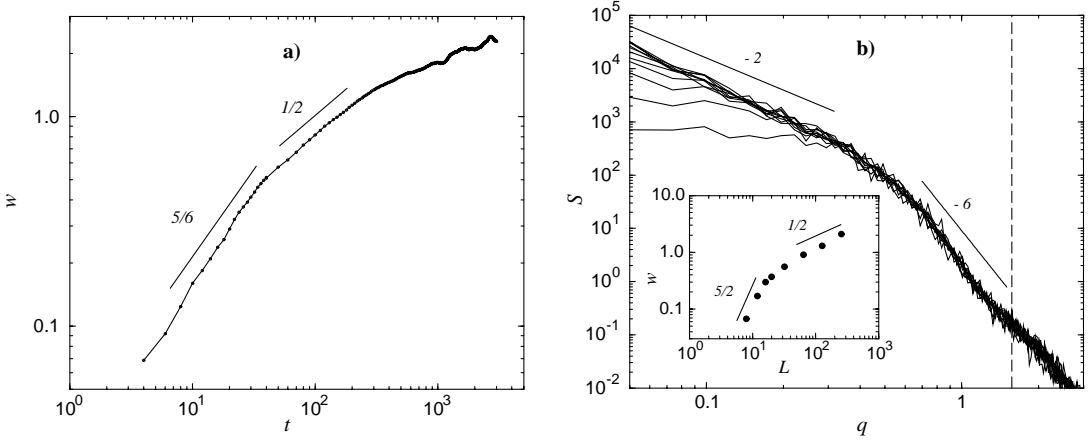


Fig. 3 – a) Temporal evolution of the interfacial width, from the numerical integration of eqs. (1), (2), for a system of size  $L = 256$ . b) Power spectrum at different time intervals, for the same case as (a). The vertical line is the spatial scale of the disorder. The interfacial width at saturation *vs.* the system size  $L$  is shown in the inset.

characteristic length in the  $y$ -direction,  $t_0 = \lambda/\bar{\gamma}_0$ . The other temporal scale corresponds to the dynamics that couples different points of the interface. For scales not much greater than  $\lambda$  this dynamics is diffusive. The associated temporal scale is the time required by the diffusion along the interface to reach distances of the scale of the disorder, and is given by  $t_D = \lambda^2/K$ . Here, we consider  $t_0 \gg t_D$ . This condition is fulfilled if  $\lambda \ll K/\bar{\gamma}_0$ . In this limit, the noise appears as persistent in the  $y$ -direction at scales comparable to  $\lambda$ . Therefore, we will take it as equivalent to a columnar (only  $x$ -dependent) noise. In this case, the stationary velocity  $\bar{v} = \bar{\gamma}_0 + (\bar{\gamma}_0/L) \int \xi(x) dx$ , where  $L$  is the system size in the  $x$ -direction.

In Fourier space, for small deviations from a flat interface ( $|q|h \ll 1$ ) we have

$$\frac{\partial \tilde{h}_q}{\partial t} = -K\Gamma q^2 |q| \tilde{h}_q - \bar{\gamma}_0 |q| \tilde{h}_q + \bar{\gamma}_0 \xi_q (1 - \delta_{q,0}). \quad (6)$$

We observe that short-wavelength fluctuations are damped by surface tension (first term of the r.h.s.), while long-wavelength fluctuations are damped by the advancement of the front, driven by the external flux (second term of the r.h.s.). Equation (6) leads to two different temporal regimes. The early growth regime is dominated by the first term of (6), and the dynamic exponent is  $z_1 = 3$ . By linear scaling analysis we obtain  $z - \alpha - 1/2 = 0$ , which gives  $\alpha_1 = 5/2$  and  $\beta_1 = 5/6$ . Since  $\alpha_1 > 1$ , the interface is superrough in the early time stages. At longer times the second term of (6) dominates the dynamics, and we get  $z_2 = 1$ ,  $\alpha_2 = 1/2$ , and  $\beta_2 = 1/2$ . The characteristic crossover time between the two growth regimes is given by  $t_c \sim \zeta_c^3 \sim (K\Gamma/\bar{\gamma}_0)^{3/2}$ .

We have checked these predictions by numerical integration of eqs. (1), (2) in a rectangular lattice with periodic boundary conditions in the  $x$ -direction. A constant flux  $\gamma_0$  has been maintained by fixing the value of  $\phi$  at a certain distance behind the interface (typically 20 space units). To mimic the experiments, we have assumed that the oil mobility can take two different values, so that  $\xi$  is a dichotomous noise of values  $\pm D$ . The noise is defined in boxes of side  $l_d = 4$  space units, randomly distributed with probability 0.35 for the positive value. The values of  $l_d$  and  $\gamma_0$  satisfy the requirement of noise persistence in the  $y$ -direction. Our

results for  $\gamma_0 = 0.05$ ,  $K = 1$ ,  $\epsilon = 1$  and  $D = 0.5$ , averaged over 25 realizations of the noise, are presented in figs. 3(a) and (b).

Figure 3(a) is a log-log plot of  $w(t)$ , including the analytical prediction for the growth exponents. The numerical results are consistent with a crossover between  $\beta_1 = 5/6$  at short times and  $\beta_2 = 1/2$  at longer times. Figure 3(b) shows a log-log plot of  $S(q, t)$ . At short times the spectrum displays a *plateau* for small  $q$ , followed by a power law corresponding to  $\alpha_1 \simeq 5/2$  for large  $q$ . At longer times,  $S(q, t)$  shows a data collapse at small  $q$  into a power law corresponding to  $\alpha_2 \simeq 1/2$ . The same results are obtained from the analysis of  $w$  vs. system size  $L$ , shown in the inset of fig. 3(b). We observe the predicted crossover between the two growth regimes. Using the scaling relation  $\alpha = z\beta$ , the dynamic exponents are  $z_1 \simeq 3$  at short times and  $z_2 \simeq 1$  at long times, in agreement with the analytical results.

Although we have experimental indications of very fast growth in the earliest time stages, we have not been able to identify experimentally the short-time scaling regime predicted by the model. This regime is difficult to access experimentally because it is very short, it is obscured by the transient originated by setting  $Q$  to its nominal value, and, in addition, the short-time behaviour of  $w(t)$  is strongly dependent on the definition of  $t = 0$ . Nevertheless, the experimental power spectrum shows that the short length scales saturate with a larger roughness exponent than the long length scales, which points to a different mechanism at the two scales, in the same direction as the model. The experimental and calculated values of the roughness exponent at short length scales do not coincide because the details of the physical mechanisms operative at the shortest length scales (capillary phenomena) are not properly captured by the model.

Concerning the long time and long length scaling regime, several authors have argued that FFI should fall in the KPZ universality class ( $\beta = 1/3$  and  $\alpha = 1/2$  in  $1+1$  dimensions) in the limit of large  $C_a$  considered here [4, 19]. Our experimental and theoretical results contradict this prediction for the exponent  $\beta$ , which is consistently found to be  $\beta \simeq 1/2$ . Concerning the roughening exponent  $\alpha$ , however, previous experimental measurements [4] and our own experiments give  $\alpha > 0.6$  or larger. Although the value of  $\alpha$  decreases with increasing  $C_a$ , the theoretical limit  $\alpha = 0.5$  is presumably not accessible because the saturation width  $w$  falls to magnitudes comparable to the gap thickness or to the typical pore size as  $C_a$  becomes very large.

In conclusion, we have studied the dynamics of interfacial roughening in the forced fluid invasion of a model porous medium at constant flow rate, in  $1+1$  dimensions. We have focused on displacements in which the viscous pressure field dominates over the fluctuations in capillary pressure (large  $C_a$ , weak disorder), and found a new universality class with two distinct time regimes.

\* \* \*

We acknowledge the financial support of the Dirección General de Enseñanza Superior (Spain) under projects BFM2000-0628-C03-01 and BFM2000-0624-C03-02.

## REFERENCES

- [1] MEAKIN P., *Fractals, Scaling and Growth far from Equilibrium* (Cambridge University Press, Cambridge) 1998; TAUER U. C. and NELSON D. R., *Phys. Rep.*, **289** (1997) 157; KARDAR M., *Phys. Rep.*, **301** (1998) 85.
- [2] RUBIO M. A., EDWARDS C. A., DOUGHERTY A. and GOLLUB J. P., *Phys. Rev. Lett.*, **63** (1989) 1685.
- [3] HORVATH V. K., FAMILY F. and VICSEK T., *J. Phys. A*, **24** (1991) L25.

- [4] HE S., KAHANDA G. L. M. K. S. and WONG P.-Z., *Phys. Rev. Lett.*, **69** (1992) 3731.
- [5] WONG P.-Z., *MRS Bull.*, **19** (1994) 32.
- [6] DELKER T., PENGRA D. B. and WONG P.-Z., *Phys. Rev. Lett.*, **76** (1996) 2902.
- [7] FAMILY F. and VICSEK T., *J. Phys. A*, **18** (1985) L75.
- [8] LÓPEZ J. M. and RODRÍGUEZ M. A., *Phys. Rev. E*, **54** (1996) R2189; LÓPEZ J. M., RODRÍGUEZ M. A. and CUERNO R., *Physica A*, **246** (1997) 329.
- [9] The silicone oil has kinematic viscosity  $\nu = 50 \text{ mm}^2/\text{s}$ , density  $\rho = 0.99 \text{ g/cm}^3$ , and surface tension with air  $\sigma = 20.7 \text{ mN/m}$  at room temperature.
- [10] Although the different height at the end points should ideally be attributed to long-wavelength fluctuations (small  $q$ ), we believe that in our experimental setup it is dominated by the wetting of the gap spacers by the invading oil, which changes the physics at the two ends. For this reason, we have ignored 8 mm of the interface at each of the two ends, and imposed the linear correction explained in the text. Measurements of  $w$  as a function of the size  $l$  of a local window demonstrate that the correction does not modify the measured exponents.
- [11] KRUG J. and MEAKIN P., *Phys. Rev. Lett.*, **66** (1991) 703.
- [12] GANESAN V. and BRENNER H., *Phys. Rev. Lett.*, **81** (1998) 578.
- [13] DUBÉ M., ROST M., ELBER K. R., ALAVA M., MAJANIEMI S. and ALA-NISSILA T., *Phys. Rev. Lett.*, **83** (1999) 1628; *Eur. Phys. J. B*, **15** (2000) 701; DUBÉ M., ROST M. and ALAVA M., *Eur. Phys. J. B*, **15** (2000) 691.
- [14] HOHENBERG P. C. and HALPERIN B. I., *Rev. Mod. Phys.*, **49** (1977) 435.
- [15] YEUNG C., MOZOS J. L., HERNÁNDEZ-MACHADO A. and JASNOW D., *J. Stat. Phys.*, **70** (1993) 1149; MOZOS J. L., PhD thesis (Universitat de Barcelona) 1993.
- [16] SAFFMAN P. G. and TAYLOR G. I., *Proc. R. Soc. London, Ser. A*, **245** (1958) 312.
- [17] JASNOW D. and VIÑALS J., *Phys. Rev. A*, **41** (1990) 6910.
- [18] LANGER J. S. and TURSKI L. A., *Acta Metall.*, **25** (1977) 1113.
- [19] KESSLER D. A., LEVINE H. and TU Y., *Phys. Rev. A*, **43** (1991) 4551.